The surface protein HvgA mediates group B streptococcus hypervirulence and meningeal tropism in neonates

Asmaa Tazi,[1,2,3] Olivier Disson,[4,5] Samuel Bellais,[1,2] Abdelouhab Bouaboud,[1,2] Nicolas Dmytruk,[3] Shaynoor Dramsi,[6] Michel-Yves Mistou,[6] Huot Khun,[7] Charlotte Mechler,[8] Isabelle Tardieux,[1,2] Patrick Trieu-Cuot,[6] Marc Lecuit,[4,5,9] and Claire Poyart[1,2,3,6]

[1]Institut Cochin, Université Paris Descartes Faculté de Médecine, Centre National de la Recherche Scientifique (UMR 8104), 75014 Paris, France
[2]Institut National de la Santé et de la Recherche Médicale, U1016, 75014 Paris, France
[3]Assistance Publique Hôpitaux de Paris, Service de Bactériologie, Centre National de Référence des Streptocoques, Hôpital Cochin, 75014 Paris, France
[4]Institut Pasteur, Groupe Microorganismes et Barrières de l'Hôte, 75015 Paris, France
[5]Institut National de la Santé et de la Recherche Médicale Avenir U604, 75015 Paris, France
[6]Institut Pasteur, Unité de Biologie des Bactéries Pathogènes à Gram Positif, URA Centre National de la Recherche Scientifique 2172, 75015 Paris, France
[7]Institut Pasteur, Unité d'Histotechnologie et Pathologie, 75015 Paris, France
[8]Assistance Publique Hôpitaux de Paris, Service d'Anatomie Pathologique, Hôpital Louis Mourier, 92700 Colombes, France
[9]Université Paris Descartes Faculté de Médecine, Assistance Publique-Hôpitaux de Paris, Service des Maladies Infectieuses et Tropicales, Hôpital Necker-Enfants Malades, 75015 Paris, France

Streptococcus agalactiae **(group B streptococcus; GBS) is a normal constituent of the intestinal microflora and the major cause of human neonatal meningitis. A single clone, GBS ST-17, is strongly associated with a deadly form of the infection called late-onset disease (LOD), which is characterized by meningitis in infants after the first week of life. The pathophysiology of LOD remains poorly understood, but our epidemiological and histopathological results point to an oral route of infection. Here, we identify a novel ST-17–specific surface-anchored protein that we call hypervirulent GBS adhesin (HvgA), and demonstrate that its expression is required for GBS hypervirulence. GBS strains that express HvgA adhered more efficiently to intestinal epithelial cells, choroid plexus epithelial cells, and microvascular endothelial cells that constitute the blood–brain barrier (BBB), than did strains that do not express HvgA. Heterologous expression of HvgA in nonadhesive bacteria conferred the ability to adhere to intestinal barrier and BBB-constituting cells. In orally inoculated mice, HvgA was required for intestinal colonization and translocation across the intestinal barrier and the BBB, leading to meningitis. In conclusion, HvgA is a critical virulence trait of GBS in the neonatal context and stands as a promising target for the development of novel diagnostic and antibacterial strategies.**

CORRESPONDENCE
Claire Poyart:
claire.poyart@cch.aphp.fr
OR
Marc Lecuit:
marc.lecuit@pasteur.fr

Abbreviations used: BBB, blood–brain barrier; CNS, central nervous system; EOD, early-onset disease; GBS, group B streptococcus; HvgA, hypervirulent GBS adhesin; LOD, late-onset disease; qRT-PCR, quantitative RT-PCR; TH, Todd Hewitt.

Group B streptococcus (GBS; *Streptococcus agalactiae*) is a Gram-positive encapsulated commensal bacterium of the human intestine that is also present in the vagina of 15–30% of healthy women. In neonates, it may turn into a deadly pathogen, and it is the leading cause of neonatal pneumonia, septicaemia, and meningitis (Edwards and Baker, 2005). Despite early antimicrobial treatment and improvement in neonatal intensive care, up to 10% of neonatal GBS infections are lethal, and 25–35% of surviving infants with meningitis experience permanent neurological sequelae (Edwards and Baker, 2005). GBS is also a

M. Lecuit and C. Poyart contributed equally to this paper.

© 2010 Tazi et al. This article is distributed under the terms of an Attribution–Noncommercial–Share Alike–No Mirror Sites license for the first six months after the publication date (see http://www.rupress.org/terms). After six months it is available under a Creative Commons License (Attribution–Noncommercial–Share Alike 3.0 Unported license, as described at http://creativecommons.org/licenses/by-nc-sa/3.0/).

The Rockefeller University Press $30.00
J. Exp. Med. Vol. 207 No. 11 2313-2322
www.jem.org/cgi/doi/10.1084/jem.20092594

The Journal of Experimental Medicine

significant cause of morbidity and mortality in nonpregnant adults, particularly those with underlying diseases and the elderly (Phares et al., 2008).

Two distinct GBS-associated clinical syndromes, referred to as early-onset disease (EOD) and late-onset disease (LOD) have been recognized in neonates in their first week of life (age 0–6 d) and after (age 7–89 d), respectively (Edwards and Baker, 2005). Although intrapartum antibioprophylaxis for parturient women at risk for GBS infection has markedly decreased the incidence of EOD, it did not change that of LOD (Poyart et al., 2008; CDC, 2009). Epidemiological data collected worldwide have shown that a substantial proportion of EOD and the majority of LOD are associated with capsular serotype III (Lin et al., 2006; Gherardi et al., 2007; Phares et al., 2008; Poyart et al., 2008; CDC, 2009). Strains of serotype III contain a limited number of clonal complexes, defined by multilocus sequence typing. Among them, the ST-17 sequence type is strongly associated with neonatal meningitis and was therefore designated as "the hypervirulent clone," despite the absence of experimental data to support this assertion (Musser et al., 1989; Jones et al., 2003, 2006; Brochet et al., 2006; Lamy et al., 2006; Bohnsack et al., 2008; Poyart et al., 2008; Manning et al., 2009).

For EOD, the mode of transmission in newborns is thought to be vertical, by inhalation of GBS-contaminated amniotic or vaginal fluid during parturition, followed by bacterial translocation across the respiratory epithelium and subsequent systemic infection (Edwards and Baker, 2005). In contrast, for LOD, the mode of transmission and the infection route remain elusive, although mother-to-child transmission might also be involved. A plausible scenario would involve early intestinal colonization by GBS that would lead in the first days of life to its intraluminal intestinal multiplication, translocation across the intestinal epithelium, and access to the bloodstream. Indeed, an intestinal portal of entry for LOD is supported by several lines of evidence: (a) 60 and 40% of the neonates asymptomatically colonized with GBS at birth remain positive for bacteria at the rectal level at 4 and 12 wk of life, respectively (Weindling et al., 1981); and (b) a longitudinal study of GBS vaginal and rectal colonization in women during and after pregnancy has revealed that carriers are usually colonized for up to 2 yr by a single clone, which is also frequently found in newborn feces for up to 1 yr (Hansen et al., 2004).

Once translocated in the bloodstream, GBS has the ability to cross the blood–brain barrier (BBB) and cause meningitis. Several virulence factors contribute to the pathogenesis of GBS meningitis in animal models, but nearly all of them are involved in the septicemia phase of the infection, but not in GBS adhesion to and crossing of the BBB (Maisey et al., 2008). One exception is Srr-1, a recently characterized surface glycoprotein that promotes adhesion to and invasion of human brain microvascular endothelial cells and contributes to BBB crossing in mice (van Sorge et al., 2009). This illustrates that more studies are needed to identify virulence factors of GBS, especially in regard to its meningeal tropism and its ability to trigger LOD.

Here, we have identified a novel ST-17–specific surface-anchored protein, which is highly prevalent in cases of LOD. We show that this protein which we have called hypervirulent GBS adhesin (HvgA) mediates GBS neonatal intestinal colonization and crossing of the intestinal and blood–brain barriers, leading to meningitis, which are key features of LOD.

RESULTS AND DISCUSSION

Epidemiological evidence that the ST-17 hypervirulent GBS clone is associated with LOD and neonatal meningitis

We first analyzed 651 GBS isolates referred to the French national reference center for streptococci between 2006 and 2009 from consecutive cases of invasive infection in neonates (meningitis, $n = 138$; bacteremia, $n = 166$) and in adults (meningitis, $n = 16$; bacteremia, $n = 331$). Serotype III accounts for 86.2% of strains isolated from cases of neonatal meningitis and 60.8% of neonatal bacteremia, but only 25.7% of bacteremia in adults (Table I). Serotype III is significantly associated with meningitis during EOD (79.3%; $P < 0.0001$) and LOD (88%; $P < 0.0001$; Table I). Moreover, the serotype III ST-17 clone is significantly associated with meningitis during EOD (79.3%; $P < 0.0001$) and LOD (82.6%; $P < 0.0001$), and with bacteremia during LOD (78.1%; $P < 0.0001$; Table I). In contrast, the ST-17 clone represents <12% of isolates from adult patients with bacteremia (Table I). Together, these results obtained from a total of 651 clinical strains demonstrate that ST-17 GBS strains account for >80% of neonatal meningitis, strongly suggesting an enhanced virulence of the ST-17 clonal complex in the neonatal context. These epidemiological observations thus prompted us to search for specific virulence factors of the ST-17 clone that may account for its apparent higher pathogenicity in neonates, its close association with LOD, and its meningeal tropism.

Histopathological study of a fatal case of ST-17–associated LOD

A term female infant (gestational age, 39 wk; birth weight, 3,140 g) was born by spontaneous vaginal delivery without complication. Maternal vaginal swab at 37 wk of gestation was negative for GBS. There was no premature membrane rupture and neither skin nor rectal swab of the neonate was made at delivery. The mother and her breastfed baby were discharged on day 4. On day 14 of life, the neonate developed muscular hypotonia, poor suckling, hyperexcitability, and fever. Cerebrospinal fluid and blood cultures were positive for GBS, which was later shown to belong to serotype III and clonal complex ST-17. Breast milk was not cultivated. Despite adequate antimicrobial treatment associating amoxicillin, ceftriaxone, and gentamicin, she died 8 h later and an autopsy was performed. Cultures of stool, blood, and cerebrospinal fluid, as well as colonic and brain autopsic tissue samples, were all positive for GBS. Immunohistochemistry of paraffin-embedded gut tissue samples led to the detection of GBS associated with the intestinal tissue and inside the lamina propria (Fig. 1, a and b). GBS also heavily infected meningeal tissues, with intense inflammation indicated by the massive recruitment of polymorphonuclear cells (Fig. 1, c and d). GBS was also observed to be tightly associated with brain microvessel endothelial

Table I. Serotype and ST-17 distribution of 651 GBS strains isolated from neonatal and non-pregnant adult invasive infections in France between 2006 and 2009

Type of infection	Serotype no.							ST-17 no.
	Ia	Ib	II	III	IV	V	Total	
	%							%
Neonatal meningitis	12 (8.7)	4 (2.9)	0	119 (86.2)	0	3 (2.1)	138 (100)	113 (81.9)
EOD (≤6 d)	6 (20.7)	0	0	23 (79.3)	0	0	29 (100)	23 (79.3)
LOD (≥7–89 d)	6 (5.5)	4 (3.7)	0	96 (88.1)	0	3 (2.7)	109 (100)	90 (82.6)
Neonatal bacteremia	34 (20.5)	5 (3)	6 (3.6)	101 (60.8)	3 (1.8)	17 (10.2)	166 (100)	89 (53.6)
EOD (≤6 d)	27 (29)	3 (3.2)	5 (5.4)	41 (44.1)	2 (2.2)	15 (16.1)	93 (100)	32 (34.4)
LOD (≥7–89 d)	7 (9.6)	2 (2.7)	1 (1.4)	60 (82.2)	1 (1.4)	2 (2.7)	73 (100)	57 (78.1)
Adult bacteremia	71 (21.4)	36 (10.3)	37 (11.2)	85 (25.7)	17 (5.1)	85 (25.7)	331 (100)	37 (11.2)
Adult meningitis	4 (25)	2 (12.5)	1 (6.25)	8 (50)	0	1 (6.25)	16 (100)	5 (31.3)

cells and choroid plexus epithelial cells, which constitute the blood–brain parenchyma and blood–cerebrospinal fluid barriers, respectively (Fig. 1, e–l). These bacteriological and histopathological analyses of this fatal case of LOD are consistent with the hypothesis that LOD results from the ability of GBS ST-17 to efficiently colonize the intestine, cross the intestinal barrier, and cross the BBB.

HvgA is an ST-17–specific surface-anchored protein that is overexpressed in vivo

We first analyzed whether the ST-17 clone expresses specific surface-exposed molecules that could account for enhanced adhesive properties. The comparative analysis of GBS whole-genome sequences has pinpointed several genes encoding surface components specific to the ST-17 clone (Tettelin et al., 2005; Brochet et al., 2006). In particular, we have identified mosaic variants at a single genomic locus (Lamy et al., 2006) encoding a cell wall–anchored protein, with two main variants displaying 38% overall amino acid identity, namely Gbs2018A, which is also referred to as BibA (Santi et al., 2007), and Gbs2018C, which we have shown to be strictly specific to the "hypervirulent" ST-17 clone (Lamy et al., 2006). These genes have conserved regulatory regions and encode proteins with conserved N- and C-terminal parts, but a distinct central core. Indeed, comparison of the nucleotide sequences of the two loci has revealed that only the 5′ and 3′ ends of the two genes are highly conserved, displaying >90% sequence identity, whereas their internal parts display low level (50–60%)

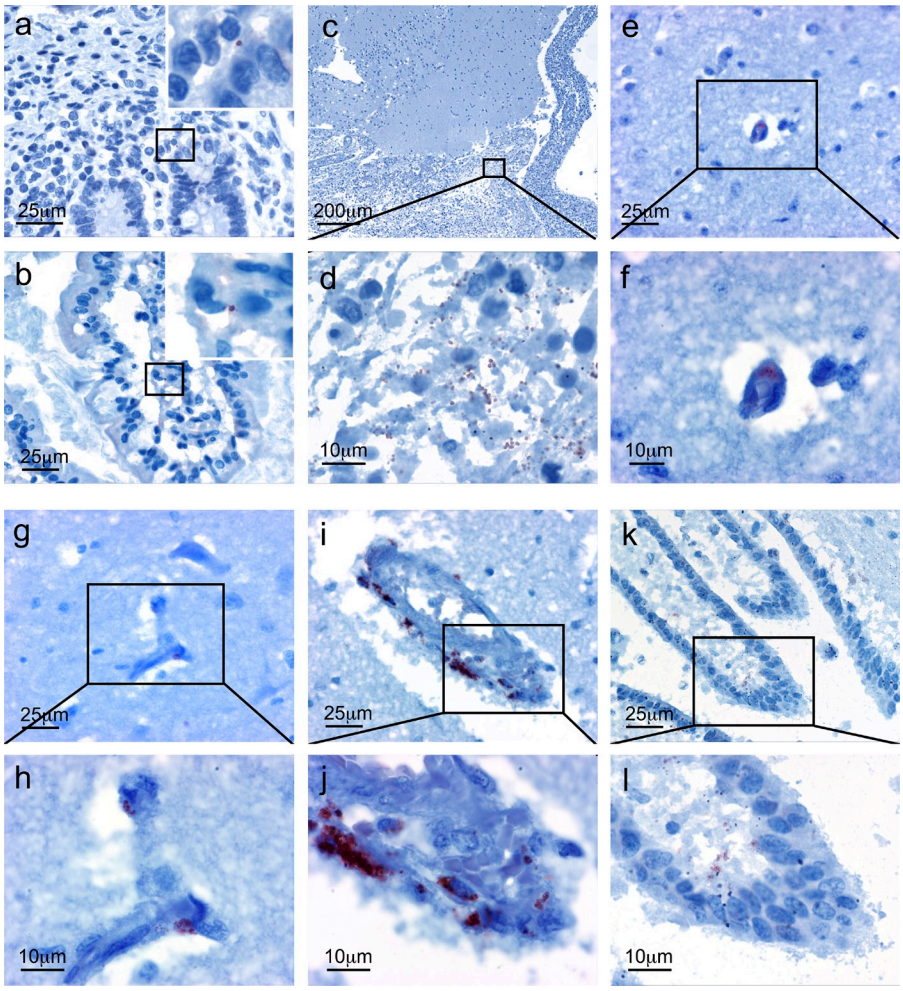

Figure 1. ST-17 GBS crossing of the intestinal and BBBs in a fatal case of human neonatal LOD with meningitis. Immunohistological study of the intestine and the CNS of a fatal case of ST-17 LOD. Bacteria were labeled with a specific polyclonal antibody to GBS and appear in reddish brown. Sections were counterstained with hematoxylin. GBS is present in the intestine (a and b), in meninges (c and d), in brain microvessels (e–j), as well as in choroid plexuses (k and l).

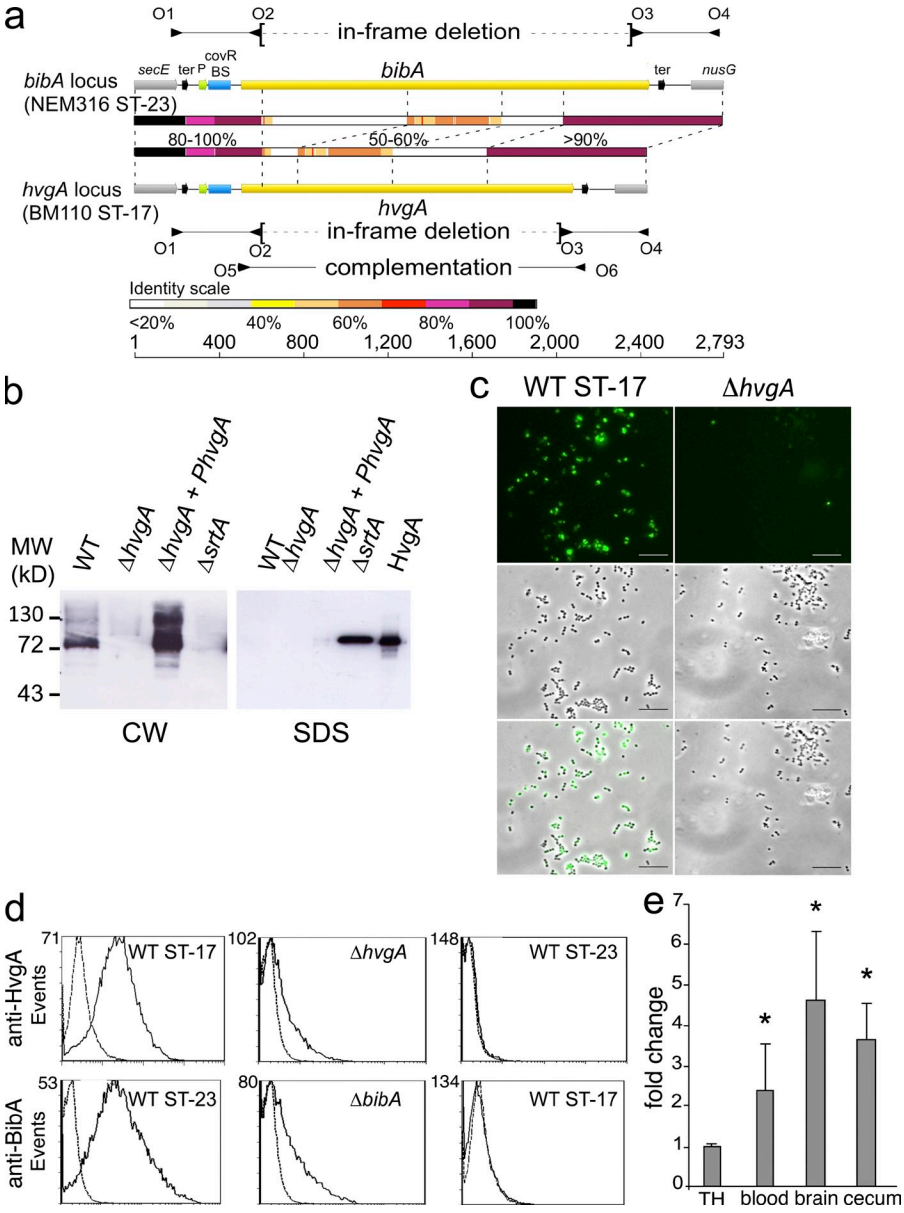

Figure 2. HvgA is a cell surface protein of GBS ST-17. (a) Structure of the *bibA*/*hvgA* locus in GBS strains NEM316 (WT ST-23) and BM110 (WT ST-17). Comparison of the nucleotide sequences of the two loci revealed that only the 5′ and 3′ ends of the two genes were highly conserved, displaying >90% sequence identity, whereas their internal parts displayed low-level (50–60%) or no significant (<20%) sequence identity. The positions of the primers used to carry out in-frame deletion within *bibA* and *hvgA* (O1-O2 plus O3-O4), or to clone *hvgA* (O5-O6), are depicted by small vertical arrows. P, promoter; ter, terminator. The CovR binding site is depicted by a blue box. The pairwise local alignment was performed with LFasta and visualize with Laln-View (http://pbil.univ-lyon1.fr/lfasta.php). (b) Western-blot analysis of cell wall–anchored proteins of GBS with anti-HvgA antiserum. Surface proteins extracted by mutanolysin (CW) or hot SDS treatment from GBS BM110 WT ST-17, its Δ*hvgA* and Δ*srtA* mutants, and the complemented Δ*hvgA* mutant were separated on 10% tris-glycine SDS-PAGE gels and immunoblotted with a specific anti-HvgA antiserum (protein fragment 30–216). HvgA corresponds to 2 ng of purified recombinant protein extracted from *E. coli.* (c) Cell surface exposure of HvgA in GBS WT ST-17. Immunofluorescence analysis was performed with rabbit polyclonal anti-HvgA antibodies (protein fragment 30–216) revealed with an anti-IgG coupled to Alexa Fluor 488. Bars, 10 µm. (d) Flow cytometry analysis of GBS WT ST-17 and its Δ*hvgA* mutant, GBS WT ST-23 and its Δ*bibA* mutant incubated with a polyclonal anti-HvgA, or anti-BibA (protein fragment 34–295) antibodies and stained with a secondary Alexa Fluor 488–conjugated anti-rabbit IgG antibody (solid line) or with secondary only (dotted line). (e) qRT-PCR analysis of *hvgA* in GBS BM110 in vitro and in vivo. Values are presented as a ratio of expression in blood, brain, and cecum of infected BALB/c mice relative to expression in TH broth medium. Results shown are representative of two independent experiments performed in triplicate. Error bars are the SD of the depicted variable. *, $P < 0.05$.

or no significant (<20%) sequence identity (Fig. 2 a). We thus investigated the contribution of Gbs2018C (hereafter named HvgA for hypervirulent GBS adhesin) to GBS neonatal infection using in vitro and in vivo approaches, with the hypothesis that it might be responsible for enhanced virulence capacities of the ST-17 clone. We first demonstrated, by immunoblotting using specific anti-HvgA antibodies that HvgA in GBS BM110, a prototype ST-17 strain, harbors an LPXTG motif that anchors it to the cell wall in a sortase A–dependent manner. As shown in Fig. 2 b, a band corresponding to HvgA was detected in cell wall extracts of the WT strain, but not of an isogenic Δ*srtA* mutant strain. Analysis of the corresponding culture supernatant demonstrated that this protein is not secreted in the medium by the WT strain (unpublished data). Moreover, after incubation in SDS at high temperature (10 min at 100°C), HvgA is massively released in the culture supernatant of the Δ*srtA* mutant, but not of the WT GBS BM110. Collectively, these results demonstrate that HvgA is a protein anchored to the cell wall by sortase A. Flow cytometry and immunofluorescence microscopy confirmed surface expression of HvgA in GBS WT ST-17 (Fig. 2, c and d). To investigate *HvgA* expression in vivo, quantitative RT-PCR (qRT-PCR) on mRNAs extracted from cecal, blood, and brain samples of orally or i.v. infected mice (see Materials and methods) were performed and demonstrated that *hvgA* in vivo expression, relative to that of *rpoB,* is two- to fourfold higher than in vitro (Fig. 2 e). Moreover, in total

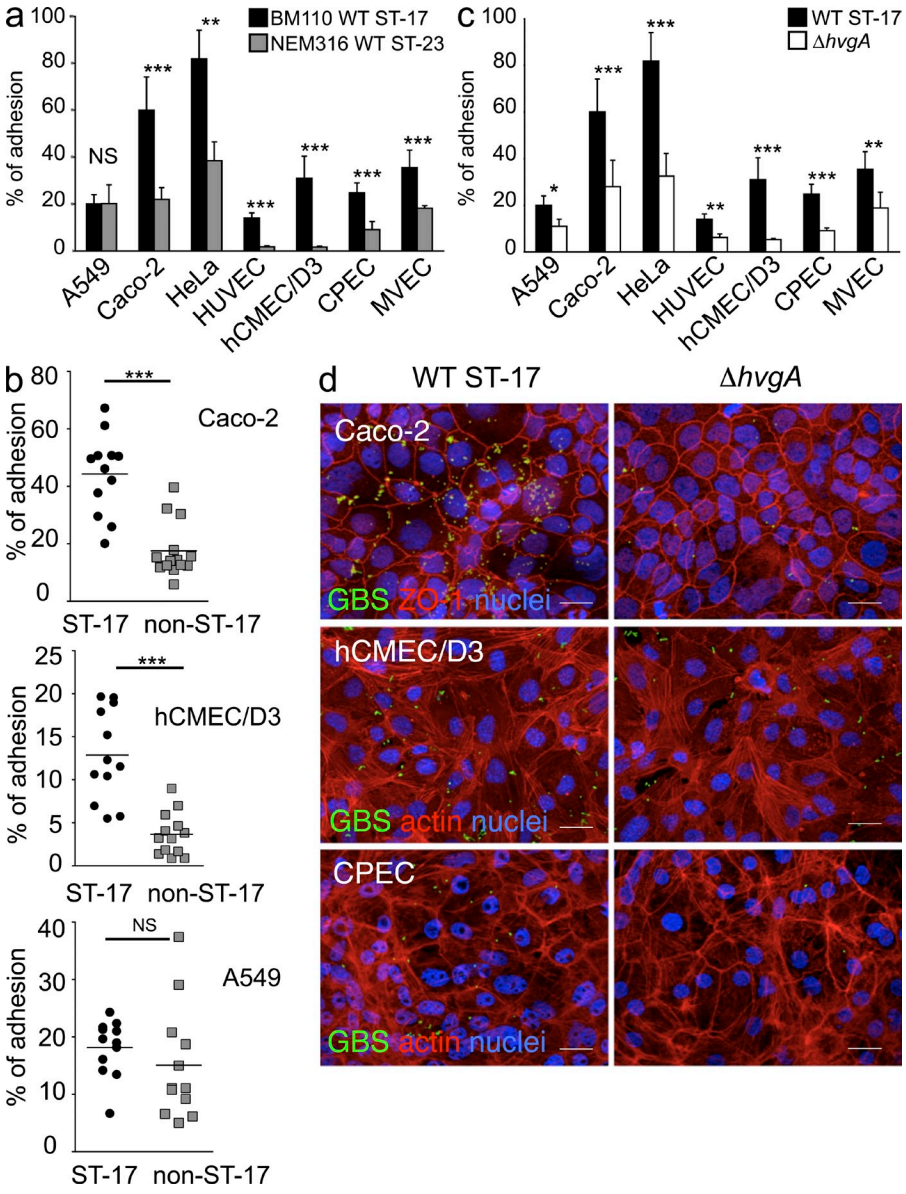

Figure 3. HvgA promotes specific hyper-adhesion to epithelial and endothelial cells. (a and b) Comparison of the adhesive properties of ST-17 and non–ST-17 GBS strains. Cells were cultured for 1 h with bacteria, washed three times, and lysed, and CFUs were enumerated after plating on TH agar plates. Values are expressed as the percentage of adhesion relative to the inoculum. (c and d) Adhesion of GBS BM110 WT (ST-17) and *Δhvg*A mutant to various cell lines, primary choroid plexus epithelial cells, and brain microvessel endothelial cells. Adhesion assays were conducted as described in a and b. Streptococci were labeled with a pAb-GBS (green), nuclei were labeled with Dapi (blue) and ZO1 with an anti-ZO1 antibody, and F-actin was labeled with phalloidin (red). Bar, 20 µm. Throughout this figure, results are representative of at least three independent experiments performed in triplicate. Error bars represent the SD. Asterisks indicate significant differences relative to BM110 WT or GBS ST-17 strains, as assessed by the Mann-Whitney test (*, $P < 0.05$; **, $P < 0.01$; ***, $P < 0.001$). NS, a nonsignificant difference.

human blood, *hvgA* is similarly overexpressed by threefold relative to standard culture medium (unpublished data). As for *gbs2018A/bibA* (Lamy et al., 2004; Mereghetti et al., 2008), *hvgA* transcription is up-regulated 85-fold in a 2-component regulatory system CovSR mutant (BM110*ΔcovR*; unpublished data). Together, these data show that HvgA is expressed on GBS ST-17 surface and that its expression is up-regulated in in vivo conditions.

HvgA promotes specific GBS adhesion to epithelial and endothelial cells

Because these data pointed to HvgA as a potential ST-17–specific determinant conferring selective adhesive properties to GBS, we compared the adhesion to different cell types of two reference strains, BM110 serotype III ST-17 (WT ST-17) and NEM316 serotype III ST-23 (WT ST-23) expressing HvgA and BibA, respectively (Table S1). Whereas both strains adhere similarly to A549 pulmonary epithelial cells, the ST-17 strain adheres significantly more efficiently to the intestinal epithelial Caco-2 cell line, the BBB-constituting cells hCMEC/D3, brain primary microvessel endothelial cells (MVECs), and choroid plexus epithelial cells (CPECs; Fig. 3 a). The significance of these results was broadened by the study of 20 randomly picked invasive GBS neonatal isolates of ST-17 type ($n = 10$) or non–ST-17 type ($n = 10$; strain characteristics described in Table S2). As seen for the prototype strains, comparative cell binding assays showed that ST-17 isolates adhere significantly more to Caco-2 and hCMEC/D3 cells than non–ST-17 isolates, but not to A549 cells (Fig. 3 b), thereby suggesting that bacteria expressing HvgA could display a specific enhanced capacity to adhere to cells of the intestinal and blood–brain barriers. To further investigate whether HvgA is the adhesin involved in the ST-17 interaction with intestinal and blood–brain barriers constituting cells, a GBS BM110*ΔhvgA* deletion mutant was constructed (Fig. 1 a and Tables S1 and S3). As expected, HvgA was not expressed in this mutant and not detected at the bacterial cell surface (Fig. 2, b–d). The growth characteristics and the viability of the mutant in various culture media (Todd-Hewitt, RPMI, or DME complemented with 10% human serum), in total human blood, as well as the morphological characteristics and the aggregative properties

of the streptococcal chains, were similar to that of the parental WT strain (unpublished data). We then compared the adhesion properties of the Δ*hvgA* mutant to its isogenic parent, and showed that it exhibited a significantly reduced adhesion to a series of epithelial and endothelial human cell lines and rodent primary cells (Fig. 3, c and d). The direct involvement of HvgA in bacterial adhesion to cells was further established. Indeed, trans-complementation with a plasmid-driving *hvgA* expression (P*hvgA*) restored BM110Δ*hvgA* strain adhesive properties to a level similar to that of the WT strain (Fig. 4 a). Furthermore, introduction of P*hvgA* in *Lactococcus lactis* enabled HvgA expression on the lactococcal surface, as assessed by immunofluorescence microscopy and flow cytometry(Fig. 4, b and c). Trans-complemented *L. lactis* strains were used in assays as described for GBS to investigate HvgA-mediated adhesion: a strain expressing HvgA adhered significantly more efficiently to Caco-2 and hCMEC/D3 cells than *L. lactis* with a vector without insert and *L. lactis* expressing BibA (Fig. 4 d). The nonpathogenic species *L. lactis* is intrinsically nonadhesive, yet heterologous expression of HvgA in *L. lactis* confers a clear adhesive phenotype. Moreover, a Δ*bibA* mutant expressing HvgA adhered 10-fold more efficiently to hCMEC/D3 cells, as compared with the WT non–ST-17 (NEM316) strain (Fig. 4 e). Thus, replacement of *bibA* by *hvgA* in GBS NEM316 confers an ST-17 adhesion phenotype to this non–ST-17 strain, and establishes the specific adhesive property conferred upon HvgA expression.

HvgA is critical for GBS intestinal colonization and translocation across the intestinal barrier

These in vitro data argued for a key contribution of HvgA in the ability of ST-17 GBS to adhere to cells constituting the intestinal and blood–brain barriers, which are targeted during LOD. We investigated this issue in the in vivo context and used mouse models of GBS infection closely mimicking the pathology observed in the human neonate. We first monitored fecal shedding after oral inoculation (10^{10} CFUs) of Swiss female mice (3–4 wk old) with WT ST-17 (BM110), its isogenic mutant Δ*hvgA* or WT ST-23 (NEM316), to assess their respective ability to colonize the intestine. Quantification of GBS in feces showed that: a WT ST-17 strain establishes in the intestine more than one order of magnitude better than a non–ST-17 strain (Fig. 5 a), HvgA strongly contributes to this ST-17–specific phenotype (Fig. 5 b), and the non–ST-17 allelic variant BibA has no significant impact on gut colonization (Fig. 5 c). Ex vivo experiments with cecal tissue explants also demonstrated an HvgA-mediated bacterial association to the cecal epithelium (Fig. 5 d). In addition, competition experiments for intestinal colonization in which 5×10^9 CFUs of each strain were simultaneously inoculated indicated that within <1 wk, ST-17 WT totally out-competes a non–ST-17 WT strain (Fig. 5 e), as well as an isogenic Δ*hvgA* mutant (Fig. 5 f). Together, these results demonstrate that HvgA confers a selective advantage at this initial step of infection.

We next addressed whether HvgA could provide the ST-17 strain with an enhanced ability to translocate across the intestinal barrier. To test this hypothesis, we used inbred BALB/c mice, as we observed that they displayed higher susceptibility than outbred Swiss mice upon oral infection. Moreover, we also observed that 4–5-wk-old mice were more resistant upon oral challenge than preweaning (15–21-d-old) BALB/c mice. We therefore inoculated orally preweaning (15–21-d-old) BALB/c mice with 10^{10} or 2×10^9 CFUs. Their mortality rate 12 h after infection was significantly decreased when inoculated with the Δ*hvgA* mutant as compared to inoculation with the WT strain (Fig. 5 g). Furthermore, 8 h

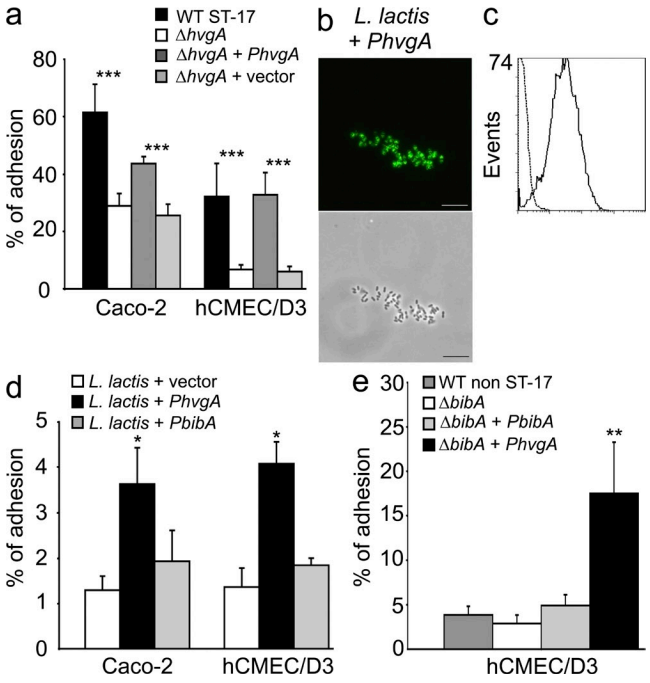

Figure 4. HvgA is necessary and sufficient to promote adhesion of GBS and *L. lactis* to epithelial and endothelial cells. (a) Comparison of the adhesive properties of WT ST-17 GBS and Δ*hvgA* mutant or complemented strain on intestinal epithelial (Caco-2) and brain microvascular endothelial (hCMEC/D3) cell lines. Adhesion assays were conducted as described for Fig. 3, performed in triplicate, and repeated independently at least 3 times; graphs show cumulative data from all experiments. Error bars represent the SD. ***, Mann-Whitney test ($P < 0.005$), relative to WT ST-17. (b and c) Expression of HvgA in *L. lactis*. (b) Immunofluorescence analysis was performed with rabbit polyclonal anti-HvgA antibodies (protein fragment 30–216) revealed with an anti-IgG coupled to Alexa Fluor 488. Bars, 10 µm. (c) Flow cytometry analysis of *L. lactis* expressing HvgA incubated with a polyclonal anti-HvgA antibody and stained with an Alexa Fluor 488–conjugated anti-rabbit IgG antibody (black line histogram). (d) Comparison of adhesive properties of *L. lactis* and HvgA- or BibA-expressing strains on Caco-2 and hCMEC/D3 cell lines. Error bars represent the SD. *, Mann-Whitney test ($P < 0.05$), relative to *L. lactis* + vector. (e) *hvgA* confers to WT non–ST-17 and ST-17 adhesion phenotype. Comparison of adhesive properties of WT non–ST-17 and Δ*bibA* mutant or complemented strains expressing BibA or HvgA on brain microvascular endothelial cell line hCMEC/D3. Experiments were performed in triplicate and repeated independently at least three times; graphs show cumulative data from all experiments. **, Mann-Whitney test ($P < 0.01$), relative to WT non ST-17.

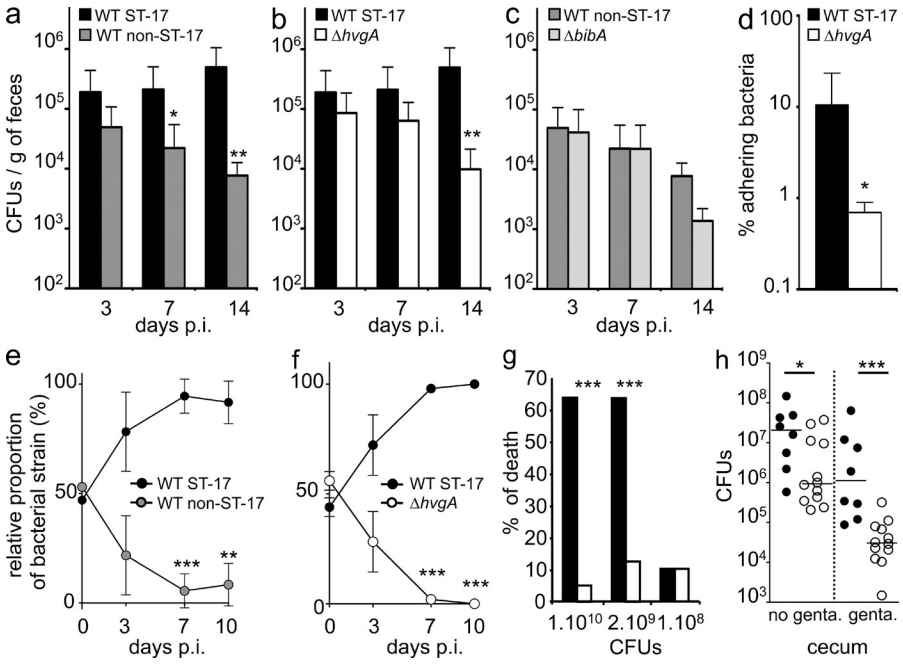

Figure 5. HvgA enables GBS persistent intestinal colonization and promotes its crossing of the intestinal barrier. (a–c) Groups (n = 6) of 3–4-wk-old Swiss female mice were infected orally with 10^{10} CFUs WT GBS or mutant strains, and fecal shedding was assessed 3, 7, and 14 d after inoculation by CFUs enumeration. Values represent fecal shedding of the six mice in a cage. (d) Infection of Swiss mice (n = 4) ligated cecum with 10^{10} GBS WT ST-17 or Δ*hvgA* mutant strain. Bacteria were recovered 1 h after infection. Values are expressed as the percentage of adhesion relative to the inoculum. (e and f) Competition assays between WT ST-17 (BM110) and WT non–ST-17 (NEM316) or Δ*hvgA* BM110 mutant. 3–4-wk-old Swiss mice (n = 6) were infected orally with a 1:1 mixture of the two strains (total dose 10^{10} CFUs). Bacteria were enumerated from the feces collected 3, 7, and 10 d after infection. (g) Mortality rate 12 h after infection of 15–21 d old BALB/c mice (n = 10) infected orally with the WT ST-17 or Δ*hvgA* mutant strains. (h) Groups of 4-wk-old BALB/c mice (n = 10) were inoculated orally with 10^{10} CFUs WT ST-17 or Δ*hvgA* mutant strains. 8 h after infection, animals were sacrificed. Cecum were collected and divided longitudinally in two parts. One half was directly homogenized: extra- and intratissular bacteria associated with the cecum were enumerated (no genta.). The second half was incubated for 3 h in DMEM containing 250 µg/ml gentamicin to kill extratissular bacteria and homogenized. Intratissular invading bacteria were then enumerated (genta.). Animal experiments represented in this figure were repeated at least two times and groups of mice contained at least five animals. Error bars represent the SD of depicted variable performed in triplicate. Asterisks indicate significant differences as assessed by the Mann-Whitney test (*, $P < 0.05$; **, $P < 0.01$; ***, $P < 0.001$).

after oral inoculation of 4–5-wk-old BALB/c mice with 10^{10} or 10^9, no mortality was observed. But here again, the WT ST-17 strain adhered to and invaded the cecal tissue more significantly than the Δ*hvgA* mutant (Fig. 5 h and Fig. S1 a), indicating a key role for HvgA in GBS ST-17 ability to cross the intestinal barrier. Moreover, in germ-free animals infected with WT GBS ST-17, bacteria could be observed adhering to the enterocytes and in the lamina propria (Fig. S1, b–e), similar to what was observed in the human previously described LOD case (Fig. 1, a and b)

HvgA contributes to GBS crossing of the blood–brain barrier and the onset of meningitis

We next analyzed HvgA contribution to central nervous system (CNS) invasion. A role for HvgA in this process was supported by results obtained with orally inoculated animals: 15–21-d-old BALB/c mice infected with the WT GBS-ST17 strain have significantly higher bacterial counts in the brain than the mice infected with the Δ*hvgA* mutant at the experiment endpoint (Fig. 6, a and b). Moreover, animals that died in the meantime are those for which bacterial counts in the brain are the highest (Fig. 6 a), arguing for a causal relationship between HvgA expression and GBS ST-17 ability to reach the CNS after oral inoculation. To investigate the onset of meningitis in these orally inoculated animals, their brains were examined by immunohistochemistry and confocal microscopy (Fig. S2). In mice with the highest WT-ST17 bacterial load (5×10^7 CFUs) in the brain, GBS were observed adhering to the inner meningeal envelopes (pia matter, Fig. S2 a) in the brain microvessel (Fig. S2 b), in the brain parenchyma (Fig. S2 c), or in the choroid plexuses (Fig. S2 d). In contrast, no bacterium was observed in mice infected with the Δ*hvgA* mutant. To focus specifically on the crossing of the BBB and bypass the HvgA phenotype at the BALB/c intestinal barrier level, we developed a CNS infection model in which preweaning 3 wk mice were infected i.v. every 12 h with a relatively low inoculum (5×10^6 CFUs) to avoid unspecific BBB opening caused by the massive systemic inflammation triggered by high bacterial loads, but to instead mimic bloodborne neonatal meningitis. Monitoring of bacterial loads in the blood and the CNS showed that whereas WT ST-17 and its Δ*hvgA* isogenic mutant induce a similar level of bacteremia 48 h after i.v. inoculation (Fig. 6 c), Δ*hvgA* is significantly impaired in its ability to invade the CNS (Fig. 6 d). In agreement with these quantitative data, real-time imaging of bioluminescent bacteria along the infectious process revealed a marked bioluminescence emission in the head of animals infected with WT ST-17 (4/4 animals), which was detectable 20 h after infection and is visible until the death of the animal, whereas merely no signal was detected in mice infected with the Δ*hvgA* mutant (Fig. 6 e). Neuropathological analysis of infected animals 48 h after i.v. inoculation disclosed an intense

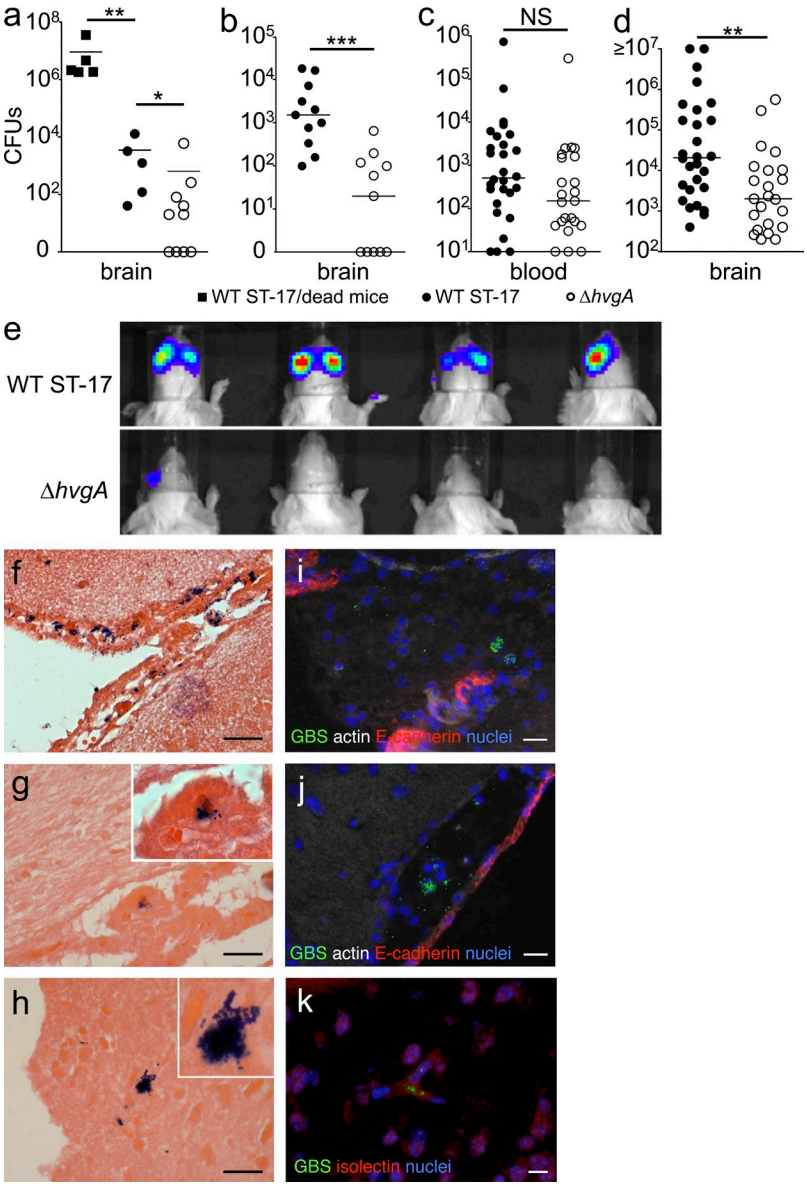

Figure 6. HvgA enables GBS crossing of the BBBs. (a and b) Groups of 15–21 d old BALB/c mice ($n > 8$) were inoculated orally with 10^9 (a) or 5×10^8 CFUs (b) WT ST-17 or *Δ hvgA* mutant strain and brain invasion was assessed 12-h after inoculation by CFUs enumeration. (c and d) Groups of 3–4-wk-old BALB/c mice ($n > 8$) were infected by repeated i.v. injections of 5×10^6 CFUs every 12 h and sacrificed at 48 h, and bacteria enumerated in blood (c) and brain (d). Data shown are the results of three independent experiments. (e) Real-time imaging of CNS infection. Groups of BALB/c mice ($n = 4$) were infected i.v. with 10^8 CFUs every 12 h. Bioluminescence was assessed every 12 h (the images shown correspond to the 36 h after injection time point). (f–h) Histopathological examination (Gram staining) of CNS tissue samples from WT-ST-17 infected mice reveals Gram-positive cocci in the meninges (f), in the choroid plexuses (g), in brain microvessel endothelial cells and the surrounding brain parenchyma (h). (i–k) Immunofluorescence staining of brain sections obtained from animals infected with the WT ST-17 in d, showing infection of meninges (i), subarachnoid space (j), and brain microvessel endothelial cells (k). Bars: (f–h) 25 µm; (i–5) 20 µm. All experiments were repeated at least three times. NS, not significant. Asterisks indicate significant differences as assessed by the Mann-Whitney test (*, $P < 0.05$; **, $P < 0.01$; ***, $P < 0.001$).

WT ST-17 streptococcal infection of choroid plexuses and meninges (Fig. 6, f, g, i, and k), as well as in brain microvessels and the surrounding brain parenchyma (Fig. 6, h and k), a result matching our observations in the human LOD case associated with ST-17 GBS (Fig. 1, c–l). Together, these in vivo results demonstrate HvgA contribution in ST-17 access to the CNS, a result that corroborates our in vitro data (Fig. 3, c and d).

Conclusions

Using complementary approaches, we have uncovered a key determinant of the pathophysiology of ST-17–associated LOD. We have identified an ST-17–specific surface-expressed protein, HvgA, and demonstrated that it is a major determinant of ST-17 hypervirulence in neonates. Our results provide a rational explanation for the two main characteristics associated with ST-17 GBS isolates: (1) their close association with LOD, which can now be linked to HvgA-mediated intestinal colonization and subsequent crossing of the intestinal barrier, and (2) their close association with meningitis, which can now be linked to the HvgA-mediated crossing of the BBB. This study definitely establishes the hypervirulence of the ST-17 GBS clone and links it to enhanced intestinal colonization and barrier breaching potentials. Importantly, it illustrates how a microbial factor implicated in bacterial intestinal colonization can behave as a specific virulence factor in the neonatal context, at a time when the intestinal microflora is not yet established and cannot exerts its buffering effect on potential pathogenic bacteria such as GBS. Given the burden of ST-17–associated LOD and neonatal meningitis (Poyart et al., 2008; CDC, 2009), *hvgA* and its gene product are now promising targets for developing diagnostic tools (Lamy et al., 2006) and vaccines (Santi et al., 2009), respectively.

MATERIAL AND METHODS

Bacterial strains, genetic constructions, and growth conditions. The main characteristics of bacterial strains and plasmids used in this study are listed in Table S1. GBS NEM316, capsular serotype III, and MLST type ST 23, and GBS BM110, capsular serotype III, and MLST sequence type ST-17 are well-characterized isolates from human with invasive infections. GBS clinical strains from invasive infection were collected by the National Reference Center for Streptococci from 2006 and 2009. GBS mutants were constructed by in-frame deletions in *bibA* (GBS NEM316), *hvgA* (GBS BM110), and *srtA* (GBS BM110), as previously described (Dramsi et al., 2006)

using primers listed in Table S3 and Fig. 2 a. The expected in-frame deletions were confirmed by PCR and sequence analysis. Complemented GBS mutant strains and *L. lactis* expressing BibA or HvgA were constructed as follows. *bibA* and *hvgA* genes were amplified by PCR from chromosomal DNA of GBS NEM316 and BM110, respectively, using primers O5 and O6 (Fig. 2 a and Table S3) and cloned into the pOri23 shuttle vector. Recombinant plasmids P*bibA* and P*hvgA* were introduced by electroporation into GBS mutants and *L. lactis*. Unless otherwise specified, GBS and *L. lactis* were cultured at 37°C in Todd Hewitt (TH) broth or agar and antibiotics were used at the following concentrations: erythromycin, 10 $\mu g.ml^{-1}$; kanamycin, 1,000 $\mu g.ml^{-1}$.

Generation of anti-BibA and anti-HvgA rabbit polyclonal antibodies. Recombinant Gbs2018 segments were expressed and purified as follows. DNA fragments intragenic to *bibA* (nt 100–1185) and *hvgA* (nt 88–648) were produced by PCR using genomic DNA of GBS NEM316 and BM110, respectively, as templates, as well as the primers listed in Table S3. DNA fragments were digested with the appropriate enzymes and cloned into pET-26b(+) and pET2817, respectively. The resulting plasmids were introduced into *E. coli* BL21λDE3/pDIA17 for protein expression. Recombinant proteins were purified under native conditions on Ni-NTA columns (QIAGEN), followed by Q–Sepharose anion exchange chromatography (GE Healthcare). The purified BibA or HvgA truncated proteins were injected into rabbit to produce antibodies, as previously described (Lalioui et al., 2005).

RNA isolation, reverse transcription, and qRT-PCR. Total RNAs were extracted from bacteria as previously described (Lamy et al., 2004). For isolation of bacterial RNA from human blood, bacteria were grown in TH broth to the mid-logarithmic phase (OD_{600nm} 0.3–0.4), washed in PBS, and resuspended in an equal volume of freshly drawn human blood from non-immune healthy donors and incubated for 1 h at 37°C. RNA isolation from animal blood and tissues was as previously described (Oggioni et al., 2006). cDNA synthesis was performed on DNase-I–treated RNA (50 ng of two independent extracts) with specific reverse primers using SuperScript II reverse transcription (Invitrogen). qRT-PCR analysis was performed as previously described (Yamamoto et al., 2005) using primers listed in Table S3. The relative fold change of each gene was calculated from $2^{-\Delta\Delta Ct}$ by using *rpoB* as an internal control gene.

Immunoblots and bacterial immunofluorescence stainings. For analysis of HvgA expression, cell wall proteins were extracted as previously described (Dramsi et al., 2006, Lalioui et al., 2005). After SDS-PAGE, proteins were transferred to nitrocellulose membrane. HvgA was detected using rabbit-specific pAb and horseradish peroxidase–coupled anti–rabbit secondary antibodies and the ECL Reagent (GE Healthcare). Immunofluorescence staining and fluorescence-activated cell sorter analysis were carried out as previously described (Dramsi et al., 2006).

Cell cultures assays. Human epithelial (Caco-2, A549, and HeLa), and human endothelial (HUVEC) cell lines are from the American Type Culture Collection. Human brain endothelial cell line hCMEC/D3 (Weksler et al., 2005) was provided by P.O. Couraud (Institut National de la Santé et de la Recherche Médicale, 75014 Paris, France). Primary choroid plexuses and brain microvascular endothelial cells were obtained, purified, and cultured as previously described (Strazielle and Ghersi-Egea, 2000; Perrière et al., 2005). Adherence assays were performed as described previously (Dramsi et al., 2006). The percentage of adherence was calculated as follows: (CFU on plate count/CFU in original inoculum) × 100.

Animal experiments. Swiss or BALB/c 2–4-wk-old female mice were used. 3–4-wk-old Swiss female mice were used for colonization assays. 15–21-d-old BALB/c female mice were used to study the mortality induced by the WT ST-17 and the translocation of the bacteria across the gut and brain barriers at earlier time points (8 or 12 h after infection).

Oral infections were as follows: 200 µl of bacterial culture was mixed with 0.3 ml of PBS containing 50 mg/ml^{-1} of $CaCO_3$ (Sigma-Aldrich) and injected intragastrically. At the indicated times, cecum were collected, rinsed in DME, and divided in two parts longitudinally. One half was directly homogenized in PBS with a tissue homogenizer. The second half was incubated for 3 h in DME containing 250 $\mu g/ml^{-1}$ gentamicin to determine bacterial invasion, rinsed, and homogenized. Serial dilutions were plated on selective medium (Granada) for CFU counts. For cecum-ligated loop experiments, animals were anesthetized. The whole cecums were closed at both ends with surgical sutures. 200 µl of the adequate bacterial dilution was injected in the lumen. 1 h after infection, the mice were sacrificed; the cecum-ligated loops were excised and opened longitudinally. For competitive assay, both WT and isogenic mutants were mixed in a 1:1 ratio oral infection experiments. At the indicated times, stools were collected and serial dilutions were plated on selective medium. i.v. infections were performed by i.v. injection every 12 h for 36 h. All of the procedures were in agreement with the guidelines of the European Commission for the handling of laboratory animals, directive 86/609/EEC (http://ec.europa.eu/environment/chemicals/lab_animals/home_en.htm) and were approved by the Animal Care and Use Committees of the Institut Pasteur.

Bioluminescence real-time imaging. GBS WT-ST17 strain and the Δ*hvgA* isogenic mutant were made bioluminescent after introduction plasmid pTCVlux by electroporation (Table S1). After i.v. infection, BALB/c mice bioluminescence was monitored each day, as previously described (Disson et al., 2009). 12 h before infection and every 12 h during the infection, animals were treated with erythromycin (20 mg/kg^{-1}).

Tissue labeling. Thin sections, thick sections, and whole-mount tissue labeling were performed as previously described (Disson et al., 2009). Acquisition of images was realized with an upright confocal microscope (Carl Zeiss, Inc.), using a 40× water immersion objective for the whole-mount tissue or an oil immersion objective for the thick section labeling. Reconstructions were realized using Imaris software.

Online supplemental material. Fig. S1 shows the role of HvgA in the crossing of the intestinal barrier. Fig. S2 shows that GBS ST-17 crosses the BBB upon oral inoculation. Table S1 describes the bacterial strains and plasmids used in this study. Table S2 describes the origin, the serotype, and the ST of GBS strains used in this study. Table S3 shows the list of primers used for genetic constructions and qRT-PCR. Online supplemental material is available at http://www.jem.org/cgi/content/full/jem.20092594/DC1.

We are grateful to Alexandra Gruss for helpful discussion and critical reading of the manuscript. We thank Pierre-Olivier Couraud for providing HCMEC/D3 cells.

This work was supported by the Agence Nationale de la Recherche (ANR HyperVirGBS Project; ANR-08-MIE-015), Institut National de la Santé et de la Recherche Médicale, Institut Pasteur, Fondation pour la Recherche Médicale (FRM), Université Paris Descartes, the Institut de Veille Sanitaire, Programme Transversal de Recherche #190. S. Bellais was a recipient of a post-doctoral fellowship from the ANR-08-MIE-015 grant and O. Disson from FRM and Institut National de la Santé et de la Recherche Médicale.

The authors declare that they have no competing financial interest.

Submitted: 4 December 2009
Accepted: 9 September 2010

REFERENCES

Bohnsack, J.F., A. Whiting, M. Gottschalk, D.M. Dunn, R. Weiss, P.H. Azimi, J.B. Philips III, L.E. Weisman, G.G. Rhoads, and F.Y. Lin. 2008. Population structure of invasive and colonizing strains of *Streptococcus agalactiae* from neonates of six U.S. Academic Centers from 1995 to 1999. *J. Clin. Microbiol.* 46:1285–1291. doi:10.1128/JCM.02105-07

Brochet, M., E. Couvé, M. Zouine, T. Vallaeys, C. Rusniok, M.C. Lamy, C. Buchrieser, P. Trieu-Cuot, F. Kunst, C. Poyart, and P. Glaser. 2006. Genomic diversity and evolution within the species *Streptococcus agalactiae*. *Microbes Infect.* 8:1227–1243. doi:10.1016/j.micinf.2005.11.010

Centers for Disease Control and Prevention (CDC). 2009. Trends in perinatal group B streptococcal disease - United States, 2000-2006. *MMWR Morb. Mortal. Wkly. Rep.* 58:109–112.

Disson, O., G. Nikitas, S. Grayo, O. Dussurget, P. Cossart, and M. Lecuit. 2009. Modeling human listeriosis in natural and genetically engineered animals. *Nat. Protoc.* 4:799–810. doi:10.1038/nprot.2009.66

Dramsi, S., E. Caliot, I. Bonne, S. Guadagnini, M.C. Prévost, M. Kojadinovic, L. Lalioui, C. Poyart, and P. Trieu-Cuot. 2006. Assembly and role of pili in group B streptococci. *Mol. Microbiol.* 60:1401–1413. doi:10.1111/j.1365-2958.2006.05190.x

Edwards, M.S., and C.J. Baker. 2005. Group B streptococcal infections. *In* Infectious diseases of the fetus and newborn infant. R. J.S, and K. J.O., editors. Saunders, 1091-1156.

Gherardi, G., M. Imperi, L. Baldassarri, M. Pataracchia, G. Alfarone, S. Recchia, G. Orefici, G. Dicuonzo, and R. Creti. 2007. Molecular epidemiology and distribution of serotypes, surface proteins, and antibiotic resistance among group B streptococci in Italy. *J. Clin. Microbiol.* 45:2909–2916. doi:10.1128/JCM.00999-07

Hansen, S.M., N. Uldbjerg, M. Kilian, and U.B. Sørensen. 2004. Dynamics of *Streptococcus agalactiae* colonization in women during and after pregnancy and in their infants. *J. Clin. Microbiol.* 42:83–89. doi:10.1128/JCM.42.1.83-89.2004

Jones, N., J.F. Bohnsack, S. Takahashi, K.A. Oliver, M.S. Chan, F. Kunst, P. Glaser, C. Rusniok, D.W. Crook, R.M. Harding, et al. 2003. Multilocus sequence typing system for group B streptococcus. *J. Clin. Microbiol.* 41:2530–2536. doi:10.1128/JCM.41.6.2530-2536.2003

Jones, N., K.A. Oliver, J. Barry, R.M. Harding, N. Bisharat, B.G. Spratt, T. Peto, and D.W. Crook; Oxford Group B Streptococcus Consortium. 2006. Enhanced invasiveness of bovine-derived neonatal sequence type 17 group B streptococcus is independent of capsular serotype. *Clin. Infect. Dis.* 42:915–924. doi:10.1086/500324

Lalioui, L., E. Pellegrini, S. Dramsi, M. Baptista, N. Bourgeois, F. Doucet-Populaire, C. Rusniok, M. Zouine, P. Glaser, F. Kunst, et al. 2005. The SrtA Sortase of *Streptococcus agalactiae* is required for cell wall anchoring of proteins containing the LPXTG motif, for adhesion to epithelial cells, and for colonization of the mouse intestine. *Infect. Immun.* 73:3342–3350. doi:10.1128/IAI.73.6.3342-3350.2005

Lamy, M.C., M. Zouine, J. Fert, M. Vergassola, E. Couve, E. Pellegrini, P. Glaser, F. Kunst, T. Msadek, P. Trieu-Cuot, and C. Poyart. 2004. CovS/CovR of group B *streptococcus*: a two-component global regulatory system involved in virulence. *Mol. Microbiol.* 54:1250–1268. doi:10.1111/j.1365-2958.2004.04365.x

Lamy, M.C., S. Dramsi, A. Billoët, H. Réglier-Poupet, A. Tazi, J. Raymond, F. Guérin, E. Couvé, F. Kunst, P. Glaser, et al. 2006. Rapid detection of the "highly virulent" group B Streptococcus ST-17 clone. *Microbes Infect.* 8:1714–1722. doi:10.1016/j.micinf.2006.02.008

Lin, F.Y., A. Whiting, E. Adderson, S. Takahashi, D.M. Dunn, R. Weiss, P.H. Azimi, J.B. Philips III, L.E. Weisman, J. Regan, et al. 2006. Phylogenetic lineages of invasive and colonizing strains of serotype III group B Streptococci from neonates: a multicenter prospective study. *J. Clin. Microbiol.* 44:1257–1261. doi:10.1128/JCM.44.4.1257-1261.2006

Maisey, H.C., K.S. Doran, and V. Nizet. 2008. Recent advances in understanding the molecular basis of group B Streptococcus virulence. *Expert Rev. Mol. Med.* 10:e27. doi:10.1017/S1462399408000811

Manning, S.D., A.C. Springman, E. Lehotzky, M.A. Lewis, T.S. Whittam, and H.D. Davies. 2009. Multilocus sequence types associated with neonatal group B streptococcal sepsis and meningitis in Canada. *J. Clin. Microbiol.* 47:1143–1148. doi:10.1128/JCM.01424-08

Mereghetti, L., I. Sitkiewicz, N.M. Green, and J.M. Musser. 2008. Extensive adaptive changes occur in the transcriptome of *Streptococcus agalactiae* (group B streptococcus) in response to incubation with human blood. *PLoS One.* 3:e3143. doi:10.1371/journal.pone.0003143

Musser, J.M., S.J. Mattingly, R. Quentin, A. Goudeau, and R.K. Selander. 1989. Identification of a high-virulence clone of type III *Streptococcus agalactiae* (group B Streptococcus) causing invasive neonatal disease. *Proc. Nat. Aca. Sci.* 86:4731–4735. doi:10.1073/pnas.86.12.4731

Oggioni, M.R., C. Trappetti, A. Kadioglu, M. Cassone, F. Iannelli, S. Ricci, P.W. Andrew, and G. Pozzi. 2006. Switch from planktonic to sessile life: a major event in pneumococcal pathogenesis. *Mol. Microbiol.* 61:1196–1210. doi:10.1111/j.1365-2958.2006.05310.x

Perrière, N., P. Demeuse, E. Garcia, A. Regina, M. Debray, J.P. Andreux, P. Couvreur, J.M. Scherrmann, J. Temsamani, P.O. Couraud, et al. 2005. Puromycin-based purification of rat brain capillary endothelial cell cultures. Effect on the expression of blood-brain barrier-specific properties. *J. Neurochem.* 93:279–289. doi:10.1111/j.1471-4159.2004.03020.x

Phares, C.R., R. Lynfield, M.M. Farley, J. Mohle-Boetani, L.H. Harrison, S. Petit, A.S. Craig, W. Schaffner, S.M. Zansky, K. Gershman, et al; Active Bacterial Core surveillance/Emerging Infections Program Network. 2008. Epidemiology of invasive group B streptococcal disease in the United States, 1999-2005. *JAMA.* 299:2056–2065. doi:10.1001/jama.299.17.2056

Poyart, C., H. Réglier-Poupet, A. Tazi, A. Billoët, N. Dmytruk, P. Bidet, E. Bingen, J. Raymond, and P. Trieu-Cuot. 2008. Invasive group B streptococcal infections in infants, France. *Emerg. Infect. Dis.* 14:1647–1649. doi:10.3201/eid1410.080185

Santi, I., M. Scarselli, M. Mariani, A. Pezzicoli, V. Masignani, A. Taddei, G. Grandi, J.L. Telford, and M. Soriani. 2007. BibA: a novel immunogenic bacterial adhesin contributing to group B Streptococcus survival in human blood. *Mol. Microbiol.* 63:754–767. doi:10.1111/j.1365-2958.2006.05555.x

Santi, I., D. Maione, C.L. Galeotti, G. Grandi, J.L. Telford, and M. Soriani. 2009. BibA induces opsonizing antibodies conferring in vivo protection against group B Streptococcus. *J. Infect. Dis.* 200:564–570. doi:10.1086/603540

Strazielle, N., and J.F. Ghersi-Egea. 2000. Choroid plexus in the central nervous system: biology and physiopathology. *J. Neuropathol. Exp. Neurol.* 59:561–574.

Tettelin, H., V. Masignani, M.J. Cieslewicz, C. Donati, D. Medini, N.L. Ward, S.V. Angiuoli, J. Crabtree, A.L. Jones, A.S. Durkin, et al. 2005. Genome analysis of multiple pathogenic isolates of *Streptococcus agalactiae*: implications for the microbial "pan-genome." *Proc. Natl. Acad. Sci. USA.* 102:13950–13955. doi:10.1073/pnas.0506758102

van Sorge, N.M., D. Quach, M.A. Gurney, P.M. Sullam, V. Nizet, and K.S. Doran. 2009. The group B streptococcal serine-rich repeat 1 glycoprotein mediates penetration of the blood-brain barrier. *J. Infect. Dis.* 199:1479–1487. doi:10.1086/598217

Weindling, A.M., J.M. Hawkins, M.A. Coombes, and J. Stringer. 1981. Colonisation of babies and their families by group B streptococci. *Br. Med. J. (Clin. Res. Ed.).* 283:1503–1505. doi:10.1136/bmj.283.6305.1503

Weksler, B.B., E.A. Subileau, N. Perrière, P. Charneau, K. Holloway, M. Leveque, H. Tricoire-Leignel, A. Nicotra, S. Bourdoulous, P. Turowski, et al. 2005. Blood-brain barrier-specific properties of a human adult brain endothelial cell line. *FASEB J.* 19:1872–1874.

Yamamoto, Y., C. Poyart, P. Trieu-Cuot, G. Lamberet, A. Gruss, and P. Gaudu. 2005. Respiration metabolism of Group B Streptococcus is activated by environmental haem and quinone and contributes to virulence. *Mol. Microbiol.* 56:525–534. doi:10.1111/j.1365-2958.2005.04555.x